IEEE Access
Multidisciplinary | Rapid Review | Open Access Journal

Received March 17, 2021, accepted March 21, 2021, date of publication March 23, 2021, date of current version April 5, 2021.

Digital Object Identifier 10.1109/ACCESS.2021.3068262

Electric Vehicle Model Based on Multiple Recharge System and a Particular Traction Motor Conception

FLAH AYMEN[1], MAJED ALOWAIDI[2] (Member, IEEE), MOHIT BAJAJ[3], (Member, IEEE), NAVEEN KUMAR SHARMA[4], (Senior Member, IEEE), SHAILENDRA MISHRA[5], (Senior Member, IEEE), AND SUNIL KUMAR SHARMA[2]

[1]PEESE, National School of Engineering of Gabès, University of Gabès, Gabès 6029, Tunisia
[2]Department of Information Technology, College of Computer and Information Sciences, Majmaah University, Al Majmaah 11952, Saudi Arabia
[3]National Institute of Technology Delhi, New Delhi 110040, India
[4]Department of Electrical Engineering, I. K. Gujral Punjab Technical University, Kapurthala 144603, India
[5]Department of Computer Engineering, College of Computer and Information Sciences, Majmaah University, Al Majmaah 11952, Saudi Arabia

Corresponding author: Sunil Kumar Sharma (s.sharma@mu.edu.sa)

This work was supported by the Deanship of Scientific Research at Majmaah University under Project RGP-2019-27.

ABSTRACT The transportation systems around the world are drastically going electrified as a trend because of inevitable heed being paid towards global warming caused by carbon dioxide emissions. A variety of equipment is contained inside these modern versions of the electrified vehicles, and many appear to be similar in types. The internal electric motor and battery power used in these designs are largely responsible for their robustness and durability in transportation systems. The energy conservation problem, on the other hand, is a vital factor that must be handled in order to ensure overall performance and cost-effectiveness. This paper provides a thorough examination of the internal equipment needed to facilitate and optimize the transportation system's energetic global success with these critical parameters. In the present study, a specific investigation is emphasized which mainly aims to recognize a new electric motor within the propulsion system. The same type of machine is discussed by elaborating internal designing through the implementation of the corresponding mathematical model and along with the corresponding electronic inverter. The associated control system is also established and implemented. Therefore, a significant theoretical contribution, made in this paper, can be used to examine the performance of a particular electrical machine for EV applications. A robust FOC-based control application confirmed this analysis. When a vehicle's power needs to be increased rapidly, this one-of-a-kind electrical machine proves its worth. Using the MATLAB simulation method, the robustness of this system's control has been demonstrated in this special mode.

INDEX TERMS Double stator- single-rotor motor, electric vehicle, field-oriented control, four-leg inverter, multiple recharge system, modeling and simulation.

LIST OF SYMBOLS

s, i, j	*The phase "i" of stator "j"*
V	*voltage*
R	*resistance*
I	*current*
q,j	*Transversal components of "j" stator*
λ_m	*Magnet flux of the rotor*
ω_{mec}	*Mechanical speed of the rotor*
$\theta_{s,j}$	*The angular position of "j" stator*
P_1	*Active power of the first stator*
$L_{s,i1\longrightarrow 1}$	*Proper inductance matrix of the first stator*
$L_{s,i1\longrightarrow 2}$	*Mutual inductance between first and second stator*
s,1	*First stator*
s,2	*Second stator*
ω	*Stator pulsation*
d,j	*Direct component of "j" stator*
Φ	*flux*

The associate editor coordinating the review of this manuscript and approving it for publication was Guijun Li.

J	*Inertia factor*
T_L	*Torque load*
θ_m	*Mechanical position*
Q_1	*Reactive power of the first stator*
$L_{s,i2\longrightarrow 1}$	*Mutual inductance between second and first stator*
$L_{s,i2\longrightarrow 2}$	*Proper inductance matrix of second stator*

I. INTRODUCTION

The planet is continuously changing by ongoing technological innovations and engineering systems are progressively becoming smarter day to day and relatively superior in their corresponding field of application. Every day, we learn about new techs, approaches and techniques to make human life relatively better. The transport sector has also been furthered by the introduction of vehicles due to the evolution of the steps. The development began in the late 17^{th} century with a steam-powered car, in the 18^{th} century with a hydrogen-powered internal combustion engine, and a petrol-powered internal combustion engine in the same century. This was mostly in the 19^{th} century. The compact model vehicle, based on an electric engine, was invented at the same time, in 1828. Ten years later, the inventor Vermont Thomas designed a DC engine, introduced the electric car, and the second but a novel one emerged. Nevertheless, following such years, the electrified variants and the regular versions had low-speeds ranging from 4 to 6 km/h. Due to the issue of restricted speed range and problems with recharging of the battery, these models could not be that successful. As a result, the gasoline-based internal combustion engine was found to be more efficient but with the problem of pollution. It was actually because of many motives, such as the lowest fuel price, the lower torque, and the slow torque. Recently, the rise in car-based ICE levels has raised the issue of emissions, and major environmental policymakers and NGO(s) have urged to minimize the use of these model cars by preferring other ecological alternatives. The electric vehicle was therefore revived, and a new policy was adopted by major governments, such as tax minimization and other benefits, to encourage the use of this type of transportation system. This has officially started after 2008, and a mass-production of electric cars came into practice. Firstly, with this strategy, the U.S. government started, followed by China and the European countries and most recently India. The latest statistics have shown that the mainstream of the new world's cars is wholly or partly dependent on electric propulsion and is still growing. This propulsion system has been developed and undergone improvements throughout history. Such propulsion systems have been designed in relation to the main source of power used. Many of them are related to combustion energy, and others are focused on renewable resources. Others have been combined to solve problems in other models, more than energy sources. The combustion-based propulsion systems have various issues related to high gas emission levels and low-speed areas where high torque is required. The engine also usually requires regular servicing, and this allows the use of this type of machine. Propulsion systems based on clean energy, such as electrical energy or hydrogen oil, have been characterized from the other side by numerous advantages referring, in particular, to the absence of any form of gas emission. The problems mentioned above, which plagued the previous combustion energy-based method, have plagued these propulsion systems.

However, the combustion engines, basing on fuel or hydrogen are characterized by two particular problems; the first problem is the high noise rates in the exhaust pipes and the second problem is related to the safety of the customer especially with the hydrogen variant. In the case of an electrical version, such problems do not exist. The underlying problem applies to the system's flexibility and the absence of a transportable energy source that can be modified for similar applications. It is evident, on the basis of the design of electric cars, that the propulsion system that uses electrical energy has numerous benefits, and that is why the number of electric vehicles in the world is rapidly growing. Some new names emerge on the world car market and manufacture electric-powered cars. The term electric vehicle has been used for any type of vehicle that uses electrical energy as its key source of power [1],[2].

For this platform, only the electric motor(s), the battery pack, and the recharge machine are practically needed inside to ensure the overall system is running. Such blocks reflect the friction and recharge components, and there are various many versions available. As a matter of fact, the traction mechanism output is related to the type of electrical motor used, if it is AC or DC, or if it is based on field windings or magnets. The type of engine used also seems to be responsible for the size of the control loop and the complexity of the electronic parts within the traction network, which provide further detail for such variants. On the other hand, the performance of the recharging system improves according to alternative recharging technologies, such as using the grid source (G2V), the photovoltaic system (PV2V), a brake regeneration system, a wireless transmitter (W2V) or using a hybrid system as a mini-ICE engine [2]. However, only three kinds of recharge methods can be used for pure electric vehicle three, as is indicated in the figure (1). In reality, if some other energy source is used within, even if it is just for the recharge phase, researchers can rule out the use of Electric Vehicles (EV). According to traditional Electric Vehicles (EV), the main versions of the world markets are based on a brushless DC system (BLDC) or a Brush-Less Alternative Current (BLAC) motor. This is due to the high rentability of the permanent magnet system and the high torque [3], [4]. There are also different solutions within the electric vehicle model. Some models are based on one electric motor; others are based on two, three, or generators. Recent versions use an electric motor inside each wheel. This approach provides more traction strength and more mobility on the roads [5], [6]. It also provides more room inside the vehicle. Nonetheless, this decreases the energy consumption ratio and increases

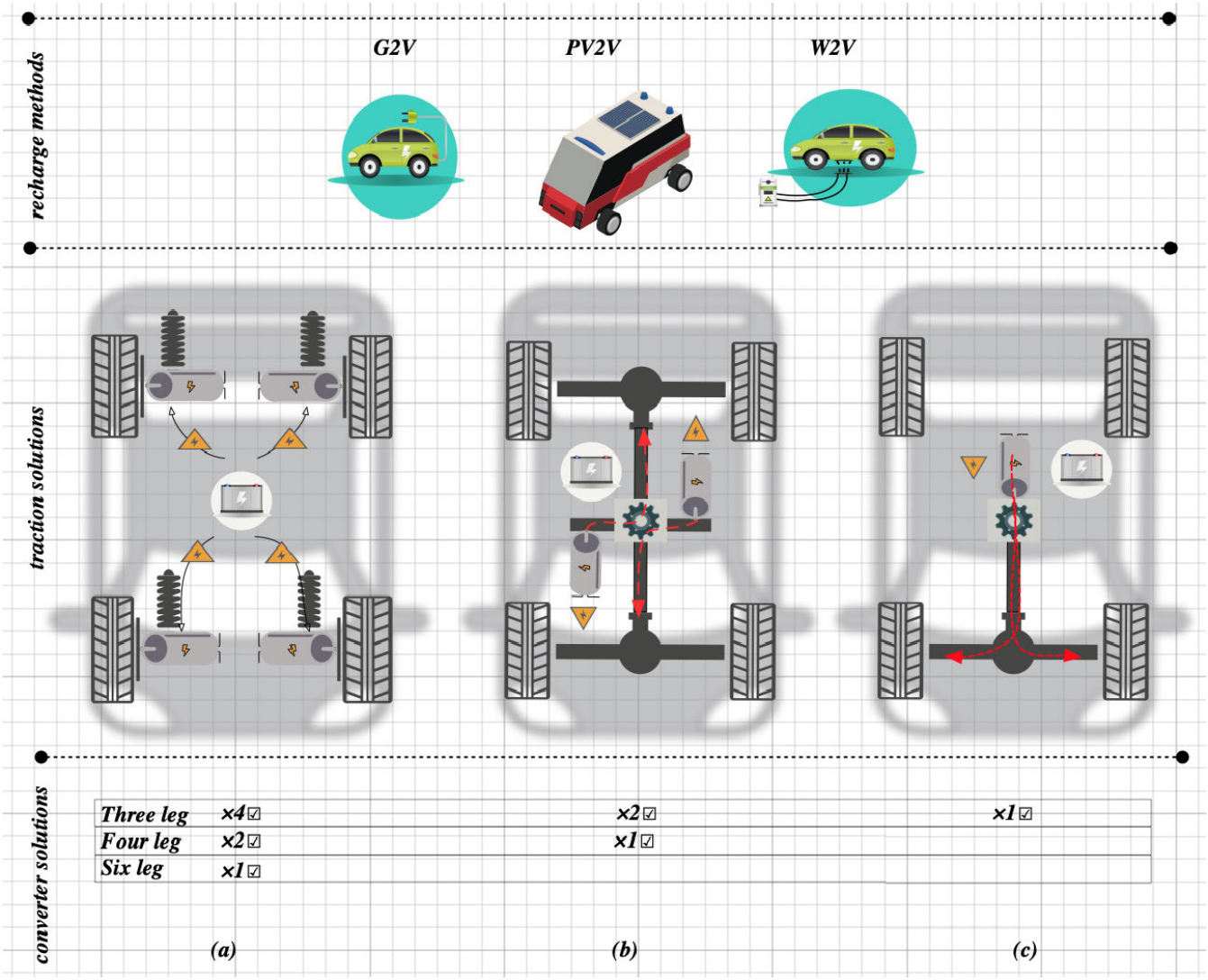

FIGURE 1. Three kinds of pure electric vehicles.

the complexity and weight of the system. Certain versions are based on only two engines, each of which is attached to the two wheels by means of a gearbox block [7]. This model was distinguished by a range of benefits, such as the flexibility of mechanical blocks and a high-starting power [8]. Figure (1) depicts three kinds of a pure electric vehicle, which based only on the electrical machine(s). Those different architectures differ in their electronic converters, who drive the motors. It is possible that each motor has its unique converter, or it is possible that every two motors have their proportional converter. Different architectures were exposed to literature in order to facilitate the electronic equipment inside the vehicle [3]–[5]. Three, four, six, or twelve legs based on DC/AC converter have appeared in order to facilitate such a problem like it is in figure (1.a) and figure (1.b), where two or more than motor was installed. As an example, for the first architecture, figure (1.a), where four motors were used, it is possible that only two converters of four legs can be used or four traditional three-phase DC/AC converters can be useful [6].

Based on these designs, certain researchers have been introduced to other specific AC machines that ensure the optimal output by using more than an electric motor inside the EV layout. Generally, the number in motors inside a pure EV increases even the desired power. However, with some special engine designs, it is conceivable that only one engine provides power equal to the sum of two different engines. Also, some special devices can offer more room inside the EV, and this is guaranteed by the required traction power [5], [6]. Double stator and double rotor machines have recently been used for friction systems, and this is due to their favorable feature of the traditional model. This research, therefore, presents a new prototype of a purely electric vehicle that uses a special motor configuration inside the traction ring. With this unique

machine design, this paper reveals the pure electrical vehicle architecture on which the propulsion system is based. Taking into account the internal requirements of this machine, this analysis introduces global mathematical models and simulates the performance of a pure electric vehicle based on this type of engine. This is achieved by displaying the effects and using the MATLAB Simulink tool. In addition, the overall block control loop is designed, identified, and applied to simulate the global traction phase process mode. This paper is, therefore, composed of five parts. In the first part, the introduction section is given. The second part is reserved for citing the blocks inside the pure electric vehicle version and their mathematical models were introduced. Next, in the third part, the required control loops are defined and explained in order to define all the necessary control steps. The fourth section is designed to check the reliability of this particular machine by checking the control loop's robustness. A special drive cycle is used to show the energetic performance of this machine and its engine capacity. The fifth part was conserved for citing the future endeavors of this work and for resume the presented work.

II. IMPORTANT COMPONENTS OF EVS

In general, every vehicle model may include a number of components. ICE is a hybrid variant of an electric car that is based on a concept or a fully electric vehicle design. In essence, there are three parts within, and they are all scheduled at the same time in all of these iterations [7], [8]. The friction part, the power supply, including the recharge system part and the extension part, comprises all other loads, such as radio, engine cooler, air conditioner, etc.

A. TRACTION SYSTEM

The traction motor forms an essential part of the electric vehicle operating mechanism. Its principal role is to give the necessary power to the wheels; the vehicle cannot be in motion without this foundation. Essentially, the electric motor with its adaptable converter is made up of all the components of this section. In the development of electric vehicles, several electrical devices have been tested and used to provide the vehicle with the required mechanical power.

Beginning with the DC machine and progressing to the AC system, modern AC machines emerge and have different patterns, unique shapes, and special interior configurations [9]. Figure (2), provides a diagram of the potential electrical equipment that can be used for the traction device and classifies it by type of voltage and displays the dates of the inventors.

Referring to a range of works of literature, new electrical machines are considered to be more suited for pure electric cars. These new machines are of smaller size, lower voltage, and lower weight. Generally, a traditional AC machine with a capacity of 50 kW can be supplemented by two special machines with a smaller size and more power than the standard one. The properties of a traditional AC machine and a special one is given in table (1) to show what we have to gain.

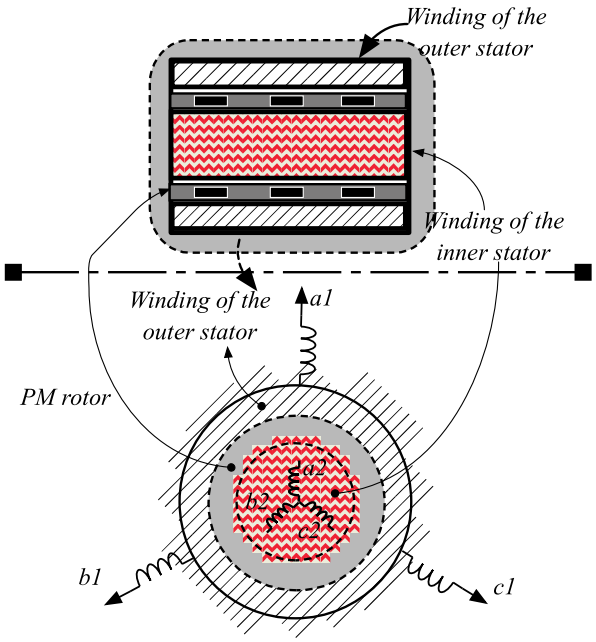

FIGURE 2. Dual stator machine: interior design.

TABLE 1. Special AC machine: proprieties and dimensions.

Electrical specifications	AC[1]	AC[2]
Torque (N.m)	362	300
Speed 10^2 rot/min	50	30
Power (kW)	32	30
Voltage(V)	480	250
Mechanical specifications		
Dimension (mm)/(mm)	L.320/ Ø.142	L.60/ Ø.250
Global Density (g/cm^3)	23.305	23.305
The Total Weight (kg)	125	60
Needed Space (Liter)	5.09	2.91

[1]: single rotor single stator Permanent Magnet machine;
[2]: dual stator single rotor Permanent Magnet machine;

1) AC ELECTRIC MOTOR: SPECIAL DESIGN FOR DOUBLE STATOR MACHINE

For its advantageous and realistic approach and hybrid architectures [13], [45], the double stator permanent magnet systems are also widely used in traction applications. This type of machine can also be found in marine traction applications [12], in the field of renewable energy [8], and it has recently been found suitable for use within vehicle wheels [13]. It was generally better suited for traction applications. This design can generate high torque at need, especially under some conditions of acceleration. It can be used inside the HEV or EV, and this motor's enabled mechanical capacity can exceed two peaks.

This machine has several solid points face the traditional machines and table (2), summarize these points and gives some classifications regarding the used electrical machines and their pros and cons.

This device can also be used as a second generator, however, which can power other external electrical components or

TABLE 2. A brief comparison between four kind of used electrical machine for HEV or EV.

	Strengths	*Weaknesses*
Simple PMSM*	• Easy to control • Simple design	• Maximal Marge of torque 300N.m • Only used as motor or a generator • High cost • High noise
Dual Stator PMSM*	• For the same size with a simple PMSM, the given torque is higher • Compact design • For the same given torque by the conventional PMSM, this motor size is smaller • Low noise	• Complex control loop • Complex design • High cost
Dual Rotor PMSM*	• Adapted for hybrid electric vehicle • High given torque • Two independent rotors	• Complex control loop • Complex design • Can't be applied for pure electric vehicle • High cost
Conventional Induction Machine	• Easy to control and Simple design	• Low given torque and speed

*PMSM : permanent magnet synchronous machine

help in charging the battery pack. So this machine can have two prototypes added. The first configuration, which consists of the larger stator used to feed the vehicle's main traction motor via a power converter. The second part, which includes the lower stator and is used by another rectifier to feed the battery system. The second design separately uses the two stators to feed the only electromagnet-force rotor. Figure (3), illustrates the second arrangement, where two converters feed the two stators independently by electric power. Another case exists, and it is where only one converter fed the two stators. Figure (2) shows in this unit the stators and designs for the rotor. This unit comprises one magnetized rotor. This rotor is positioned between the two stators, as the outer stator and the inner stator indicate [10].

The mathematical analysis of this model consists in determining the voltage vector function, as it is shown in the equation system (1).

$$\begin{cases} \textit{primary stator} \begin{cases} V_{s,a,1} = R_{s,a,1} I_{s,a,1} + \emptyset_{s,a,1} \\ V_{s,b,1} = R_{s,b,1} I_{s,b,1} + \emptyset_{s,b,1} \\ V_{s,c,1} = R_{s,c,1} I_{s,c,1} + \emptyset_{s,c,1} \end{cases} \\ \textit{secondary stator} \begin{cases} V_{s,a,2} = R_{s,a,2} I_{s,a,2} + \emptyset_{s,a,,2} \\ V_{s,b,2} = R_{s,b,2} I_{s,b,2} + \emptyset_{s,b,2} \\ V_{s,c,2} = R_{s,c,2} I_{s,c,2} + \emptyset_{s,c,2} \end{cases} \end{cases} \quad (1)$$

With $i = [a, b, c]$ and $j = [1, 2]$.

We note by V_s, R, I, and ϕ the stator voltage signal, the stator resistance the stator current and the stator flux correspondingly, for each phase "a", "b" and "c" in the first and the second stator coded by "j". We suppose that all the stator resistance for each stator is similar. We indicate that the system of flux equation is at it is expressed in equation (2) [11].

$$\phi_{s,i,j} = \begin{bmatrix} [L_{s,i1 \longrightarrow 1}] & [L_{s,i1 \longrightarrow 2}] \\ [L_{s,i2 \longrightarrow 1}] & [L_{s,i2 \longrightarrow 2}] \end{bmatrix} \quad (2)$$

where $L_{s,i1 \longrightarrow 1}$ is the proper inductance matrix for the first stator, is the mutual inductance matrix for between the two stators. With $i = [a, b, c]$ and $j = [1, 2]$.

The conversion to Park model of the system of equation exposed in (11), is given in the system of equation (3). L_{dm} and L_{qm} are the direct and transversal mutual inductances. $\omega_{s,j}$ is the angular frequency of the first and the second stator.

$$\begin{cases} \textit{primary stator} \begin{cases} V_{d,1} = R_1 I_{d,1} - (\omega_{s,1}) \emptyset_{q,1} + \dfrac{d\emptyset_{d,1}}{dt} \\ V_{q,1} = R_1 I_{q,1} + (\omega_{s,1}) \emptyset_{d,1} + \dfrac{d\emptyset_{q,1}}{dt} \end{cases} \\ \textit{secondary stator} \begin{cases} V_{d,2} = R_2 I_{d,2} - (\omega_{s,2}) \emptyset_{q,2} + \dfrac{d\emptyset_{d,2}}{dt} \\ V_{q,2} = R_2 I_{q,2} + (\omega_{s,2}) \emptyset_{d,2} + \dfrac{d\emptyset_{q,2}}{dt} \end{cases} \end{cases} \quad (3)$$

The flux equation in the park frame is as follows;

$$\begin{cases} \emptyset_{d,j} = L_{d,j} I_{d,j} + L_m \left\| I_{d,j} \right\| + \lambda_m \\ \emptyset_{q,j} = L_{q,j} I_{q,j} + L_m \left\| I_{q,j} \right\| \end{cases} \quad (4)$$

We suppose that the cyclic mutual inductance between the two stators is unique, so it is possible to note that.

$$L_m = L_{d,m} = L_{q,m}$$

Basing on this simplification, the mechanical equations of this machine are as follows: (5) represents the speed equation [12].

$$\omega_{mec} = \frac{T_e - T_l}{(J.s + B_s)} \quad (5)$$

It is important to state that the expression of the motor torque has a variable form, and this component can be described using only the first components of the stator as it is in equation (6). But it can also be expressed using the secondary

winding currents of the secondary stator, as they are in equation (7). More detailed information on these mathematical analyzes is given in [13], [14].

$$\frac{\rho}{P}C_{em} = \left[\emptyset_{d,1}i_{d,1} - \emptyset_{q,1}i_{q,1}\right] \tag{6}$$

$$C_{em} = \frac{\frac{P}{\rho}\left[\emptyset_{d,1}i_{q,2} + \emptyset_{q,1}i_{d,2}\right]}{\left[\frac{1}{\rho} + \frac{\sqrt{L_{d1}^2+L_{q1}^2}}{L_m}\right]} \tag{7}$$

2) FOUR LEGS ELECTRONIC CONVERTER FOR DOUBLE STATOR MACHINE

The use of static converters has become an extremely broad field of engineering; as variable speed drive is rapidly being used in industrial equipment. Voltage inverters are widely used for asynchronous power motors. The analog or digital control algorithm output reflects the voltages or currents that are required at the computer terminals. The Pulse Width Modulation (Pulse Width Modulation) technique allows these outputs to be replicated by means of a direct converter from a DC voltage source. Controlling AC devices with a voltage inverter usually uses modulation techniques of pulse width to control the power switches.

Through monitoring the power transistor switches, the switching errors can be minimized. This is significantly changing the voltages given to the electric motor. On the output voltages to the device, the pulse width modulation techniques are responsible for the quality. There are multiple choices, and the choice of one depends on the type of command that can be applied to the unit, the inverter's modulation frequency, and the user's collection of harmonic constraints. Modulation theory can be achieved by different approaches, conventionally by contrasting references to a triangular equation or using a criterion-satisfying, real-time measure. The vehicle's traction control system allows it to tolerate alternating variable frequency and amplitude voltages. Three-phase voltage converters allow a system of three-phase voltages to supply the electric motor, obtained from a DC input signal. For variable-speed applications, inverters run at switching frequencies of a few kHz on small and medium power machines. [4], [15].

The inverter used in our study is a three-phase inverter with two stages of voltage, with eight switching cells (IGBT's) and eight diodes. Each inverter leg is comprised of two switching cells, each consisting of the switch with its reverse diode. The output of which correlates to the leg midpoint. The switch control signals on each arm must be identical so that the continuous supply to the inverter is not short-circuited. To guard against a short circuit, a waiting time must be imposed for the connection to close, usually called a dead time. The effect of this dead time induces voltage discontinuities resulting in fluctuations of the currents and an increase in the amplitude of the related harmonics when the line currents change direction.

In this article, this special AC machine was supplied by the four-leg voltage inverter centered on a double rotor and a single stator which operates with a variable frequency. We used the concept of two independent stator windings with only a four-leg inverter to improve motor control, thus minimizing magnetic couplings and reducing stator losses. Figure (3), illustrates the architecture of the Converter and gives haw it is possible to feed the inner and the outer stator using the height transistors combination. As it is indicated in the two parts in figure (3), the outer and the inner stator can be feeding using the transistor numbered from 5 to 8 and using the neutral point, noted "N", or by using the transistor numbered from 1 to 4 and with the same neutral point "N". The voltage equations of this type of inverter will differ during operations from the ones produced by the conventional three-phase inverter. In addition, all voltages in each arm are specified with midpoint relation (between the two capacities). Pulse width modulation (PWM) is the typical method for determining switching times (and adding positive or negative voltages). It is based on the contrast of a modulation wave "V_p" (usually a high frequency triangular "f_p" signal) with a reference wave "V_{ref}" reflecting the desired output voltage of frequency "f_{ref}."

The switching signal shall be determined from the intersection of these two signals. In the case of a three-phase inverter with four arms, there will be four control signals, one for each inverter arm [12]. The interactive modulation is characterized by its modulation index r and its modulation depth "m_a", such as:

$$\left.\begin{aligned} m_a = \frac{V_{ref}}{V_p}, r = \frac{f_p}{f_{ref}} \\ V_{i-ref} < V_p \Longrightarrow S_i = 0, \quad V_{iN} = -\frac{V_{dc}}{2} \\ V_{i-ref} > V_p \Longrightarrow S_i = 1, \quad V_{iN} = \frac{V_{dc}}{2} \end{aligned}\right\} V_{iN}$$
$$= \frac{V_{dc}}{2}(2S_i - 1), \quad with\ i = a, b, c, n \tag{8}$$

The relationship between the output voltages and the switches can be defined in equation (9). The voltage of the step can be determined by equation (10).

$$\begin{bmatrix} V_{aN} \\ V_{bN} \\ V_{cN} \\ V_{nN} \end{bmatrix} = \frac{V_{dc}}{2}\begin{bmatrix} 2S_a - 1 \\ 2S_b - 1 \\ 2S_c - 1 \\ 2S_n - 1 \end{bmatrix} \tag{9}$$

$$\begin{bmatrix} V_{aN} \\ V_{bN} \\ V_{cN} \\ V_{nN} \end{bmatrix} = \begin{bmatrix} V_{aN} \\ V_{bN} \\ V_{cN} \\ V_{nN} \end{bmatrix}\begin{bmatrix} 1 & 0 & 0 & -1 \\ 0 & 1 & 0 & -1 \\ 0 & 0 & 1 & -1 \\ 0 & 0 & 0 & 0 \end{bmatrix} \tag{10}$$

B. POWER PACK SYSTEM

The electrical transport systems are based on energy storage devices such as the battery or the supercapacitors connected inside the electric drive to the propulsion system. These sources of energy may feed the vehicle by the required power at or off departure. These devices are used in large part for the pure electric vehicle or the hybrid-electric model. This gives the main transport systems a primordial instrument.

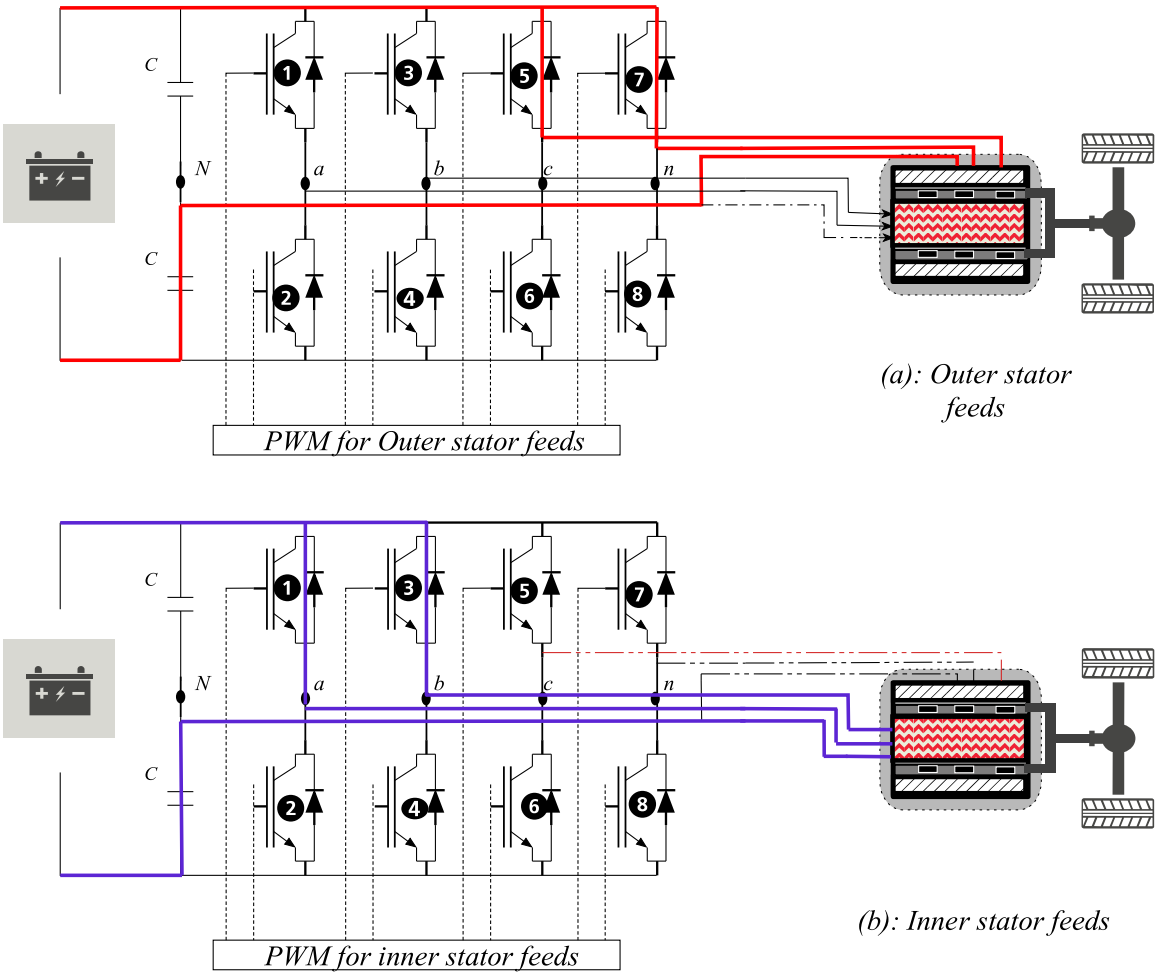

FIGURE 3. Four legs electronic converter design.

Generally defined charging or discharge mode characteristics of those mobile sources. In the case of the batteries, the question occurs in the supercapacitor face recharge time. The cycle period is generally even better in the battery case and very low for the supercapacitor case. Compared to the discharge mode, the batteries have a discharge cycle number, and the condensers are unlimited, which renders the battery's critical weaknesses. Parallel to that, the energy density may be more significant for the condensers facing batteries. It is the inverse of the criterion for power density. The efficiency of the supercapacitors is higher than the batteries for all those reasons. Those sources ' output depends on various parameters and variables.

1) BATTERY AND SUPER-CAPACITY SYSTEM

In equation (11), we show the battery output voltage, referred to as "$V_{b/cell}$" by one cell. Ultimately, the voltage expression depends on the "V_{oc}" which is the open-circuit voltage. "R_b" is a cell's ohmic resistance. "R_{st}" and "C_{st}" are the resistance and capacitance of the electromagnetic short-term double-layer properties, respectively, and "R_{lt}" and "C_{lt}" are the resistances and capacitances of the electro-chemical long-time-interval mass transport effects.

$\ll I_b \gg$ is the cell load current. As this element can be discharged or charged, $\ll$ is $\gg$ will be positive or negative, respectively.

$$V_{b/cell} = V_{oc} + R_b I_b + \int \frac{I_b - \frac{V_{st}}{R_{st}}}{C_{st}} dt + \int \frac{I_b - \frac{V_{lt}}{R_{lt}}}{C_{lt}} dt \quad (11)$$

The battery pack voltage depends on the number of serial and parallel of used cells. Equation (12), explains that relation. The battery resistance can also be found in equation (13). We indicate by "R_0", the battery cell charging or discharging resistance. With these equations, it is possible to express the battery heat generation noted "Q_{bp}" in equation (14). "ξ" is the charge efficiency. So based on the battery heat generation and basing from the initial battery temperature "T_0", it is possible to express the battery pack temperature noted "T_b" and expressed in (15). "Q_{bc}" is the heat losses, and "C_{bp}" is the battery heat capacity [16].

$$R_b N_p = (R_0 + \frac{R_{st} I_{st}}{I_l} + \frac{R_{lt} I_{lt}}{I}) N_s \quad (12)$$

$$V_b N_p = N_s V_{b/cell} \tag{13}$$

$$Q_{bp} = (R_b^2 + (1-\xi)V_b)I_b \tag{14}$$

$$T_b - T_0 = \int \frac{Q_{bp} - Q_{bc}}{m_{ba} C_{bp}} dt \tag{15}$$

The supercapacitor model, for one cell, can be visualized in equation (16). The capacity value depends, "N_e" which is the number of layers in the electrode. "ε_0" and "ε" is the permittivity of the free space and the electrolyte material. "c" presents the molar concentration and "A_i" expresses the joint area between electrodes and electrolytes. The Helmholtz layer length is "d" and "Q_c" presents the cell electric charge (C). the final capacitance value depends, the number of parallel and serial cells, noted respectively by "N_p" and "N_s", and it can be calculated as it is in equation (17). Then the outputted voltage value for the supercapacitor module can be expressed as it is in equation (18).

$$(C_{sup/cell})^{-1} = \left[\frac{d}{N_e \varepsilon \varepsilon_0 A_i} + \frac{2N_e RT}{FQ_c \sinh(\frac{Q_c}{2N_e^2 A_i \sqrt{2RT\varepsilon\varepsilon_0 c}})} \right] \tag{16}$$

$$C_{sup} N_s = N_p C_{sup/cell} \tag{17}$$

$$(V_{sup} + R_{sup} i_{sup}) C_{sup} = N_p Q_c \tag{18}$$

For supervising the batteries and the capacitors state of charge, noted $SOC_B(t)$ and $SOC_U(t)$, we can follow equation (19). $\ll \eta_I \gg$ is the Colomb efficiency at different I pack [17], [18]. "T" is the ambient temperature, and $\ll \eta_T \gg$ represents the influence coefficient of different "T" on $\ll \eta_I \gg$.

$$\begin{cases} SOC_B(t) = SOC(t_0) - \int \frac{\eta_T \eta_I I_b(t)}{Q_b} \\ SOC_U(t) = \frac{(V_{sup} - 2R_{sup} i_{sup}(t))^2}{V_{sup,max}^2} \end{cases} \tag{19}$$

2) ASSOCIATE CONVERTERS FOR POWER PACK RECHARGE

Basing on our previous presentation in the introduction section, where the possible recharge method was exposed, figure (4), exposes all the needed converters for charging the battery pack. Actually, the complexity appears in the Grid to vehicle model, where a special control loop appears. Therefore, this study concentrates on this recharge mode. More descriptions on the other recharge methods can be visualized in [7], [19], [20], [21]. The battery charger described here is composed of two power converters sharing a DC connection. One is to interface the power grid, and the other is to interface the batteries for the traction. A full-bridge AC-DC bidirectional converter is used for the interface of the power grid. During G2V operating mode, this converter can function as an active rectifier with a sinusoidal current and unitary power factor. A flexible DC-DC Converter is used to connect the batteries. This converter acts as a buck converter in G2V operating mode to control the current and voltage during the charging periods of the current and voltage batteries, respectively. Figure (4) gives the scheme of this converter.

C. MECHANICAL SYSTEM

There are various equations, related to the speed, involved in the mechanical modeling of a car. Those equation depends on the radius of the wheel, noted "r_w" and the hydraulic gear factor, noted "G" and expressed in equation (20). Secondly, the formula for vehicle speed, which can be described as in equation (20), must be articulated.

This equation is constrained by the cumulative speeds of the vehicle, and the motor stated respectively, $V_{v,max}$ and ubiquitous$_{\max}$.

$$V_v = \underbrace{\frac{w_a}{\frac{2\pi r_w \omega_{m,max}}{601.1 V_{v,max}}}}_{G} r_w \tag{20}$$

Furthermore, the vehicle torque equation "C_v" expressed is important to determine the actual force applied to the engine. This definition consists of different parameters and quantities, such as the total vehicle weight "M_v" and the road grade "Number," the road gravity "g" and the continuous traction force "f_r."

This is laid out in equation (21). With respect to vehicle weight, the weight of the engine motor, and the weight of the battery pack is applied to the weight of the chassis vehicle, as expressed in equation (22).

$$M_v \cong m_{v0} + m_{ba} + m_{em} \tag{21}$$

$$C_v = r_w (M_v g.(\sin(\theta) + f_r.\cos(\theta)) + \frac{1}{2} C_d \rho A_v V_v^2) \tag{22}$$

Previously revealed vehicle torque can help to shape the force of traction, which can be expressed as it is in equation (23). This equation depends on the area of the frontal vehicle, and the air density and the acceleration factors are given A_v, ρ and Acc have been noted.

$$F_t = M_v (g.(\sin(\theta) + f_r.(\cos(\theta)) + \rho A_v \left(\frac{V_v - V_w}{2M_v} \right) + f_m Acc) \tag{23}$$

This block will present the effect of exterior space behavior in relation to vehicle velocity and acceleration.

III. CONTROL DIAGRAMS

Several blocks are grouped together in the EV model, as previously revealed. The importance of arranging all applicable criteria and ensuring proper information flow for proper vehicle control cannot be overstated.

The overall EV function is divided into two core systems. The first is concerned with the traction mechanism, which includes the electric motor, while the second is concerned with the power source, which includes the battery pack and its recharge cycles.

Beginning with the traction step, the block of electric motors can be said to be the primary active factor in the traction process. This one appears to be in charge of regulating the

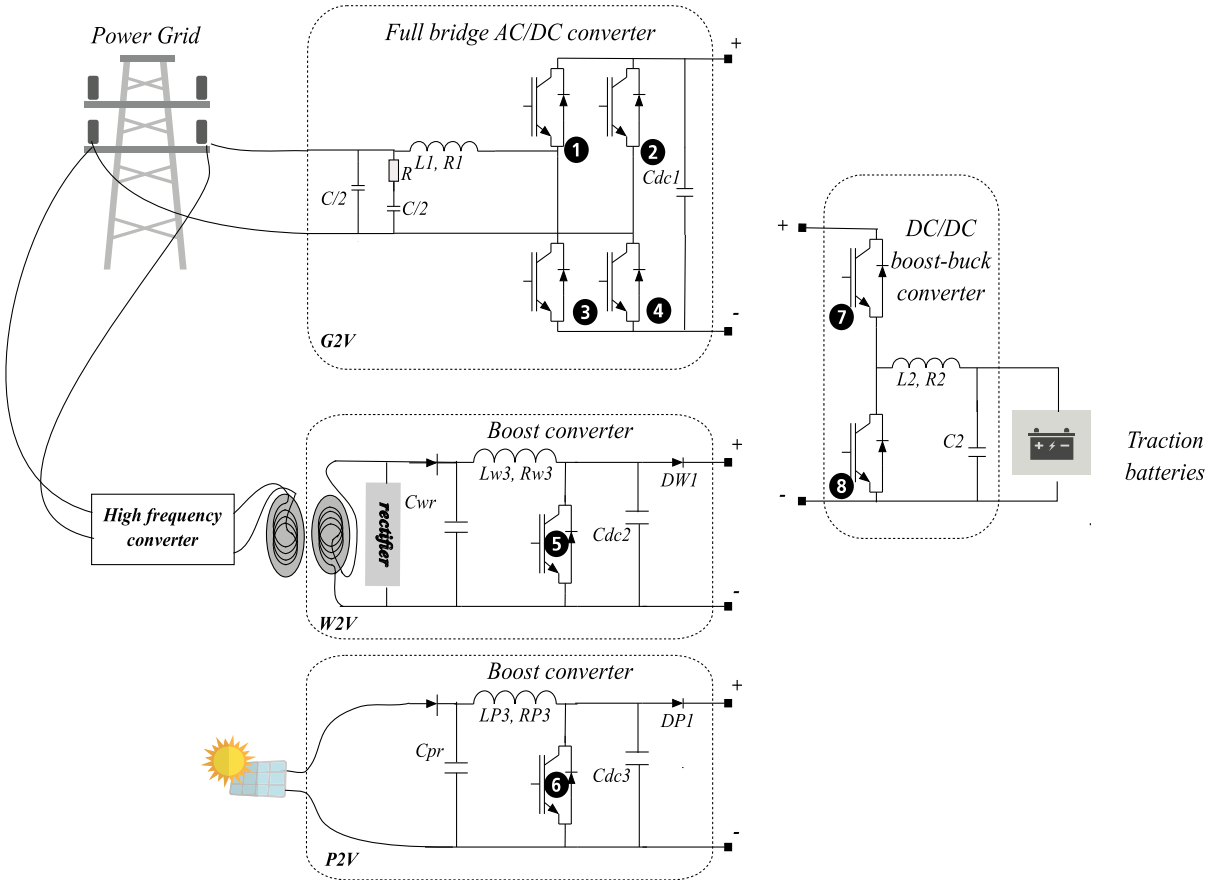

FIGURE 4. Battery charger methods and their associate converters.

vehicle's acceleration and deceleration since it is connected to the wheels via a gearbox. As indicated previously, different motor models and designs have been revealed with the literature and used to do this touch. For verifying the overall function mode of the traction phase, we desire to expose in this part the corresponding control architecture of the main sued machine, which has a special design and a special specification. Actually, this machine is not well studied in the literature, where we have found several problems for defining the corresponding control architecture. Therefore, this study explores the conventional control technic, which uses the principle of field-oriented vector control FOC. Actually, this method succeeded for controlling all AC machine and have shown high efficiency and robustness. However, as this machine has two stators, the corresponding FOC architecture will be special and have a special decoupling bloc for assuring the independence between the two-stator alimentation. More description for this control method is exposed in [14], [22], [23].

Moving to the second scheme inside the overall design of an electric vehicle, and which is the recharge system. As it is indicated previously, this study concentrates on the grid to vehicle recharge method, and therefore, in the second part in this section, we desire to expose the necessary control loop used for obtaining the goal. A control theorem based on PLL principle is designed here.

A. TRACTION SYSTEM CONTROL SCHEME

As for every AC machine, traditional control methods such as direct torque control and flow control, voltage-oriented control, and field-oriented control has been investigated; therefore, operating the dual stator system seems to be easy as it is possible to control each stator separately ()[24]. However, the control system must take into account that only one reference speed is needed and that six reference signals must be calculated. In the conventional control method, the three reference signals that will be applied to the specific stator can be produced from the reference speed. That's not the case. The control architecture must then be because follows.

Next, begin by explaining the relationship between the angels of the revolving stators and the mechanical angle expressed in the equation (24). Equation (25) describes the relationship between the electrical angles of the stators and the rotors.

$$\omega_{elem} = \frac{\omega_{s,1} + \omega_{s,2}}{(P)} \tag{24}$$

$$\theta_m = \theta_{s,1} + \theta_{s,2} \tag{25}$$

This system can be excited by either an AC or a DC current on the main or the second stator. In this case, if one of these stators is activated by a DC current, the resulting electrical angular direction is null. This case is easier to control. In our case, we are learning the form of AC excitation.

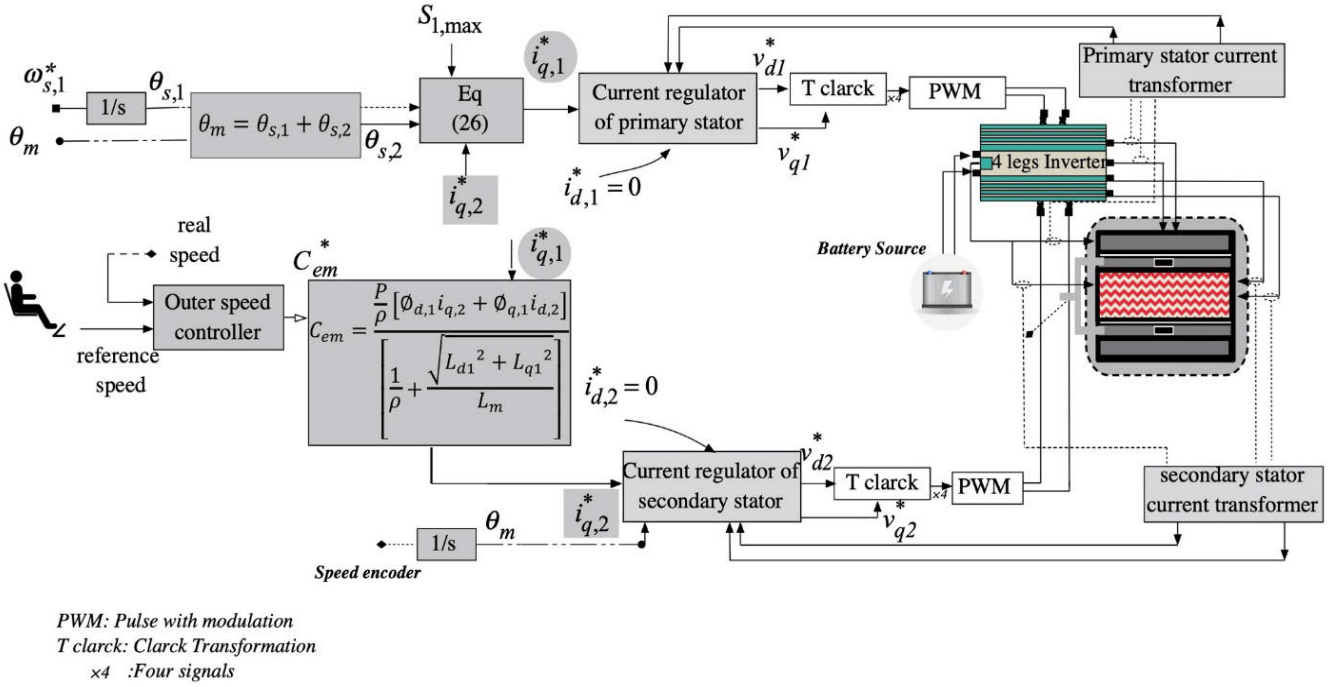

PWM: Pulse with modulation
T clarck: Clarck Transformation
×4 :Four signals

FIGURE 5. FOC loop of the dual stator machine.

The control method is based on a simple theory that required the reference currents of the primary stator and the reference speed of the rotor motor. The second reference frequency and angle will then be calculated on the basis of equations (18) and (19). By this information, the current vectors can be located on the ''dq'' frame. The PI controllers will then be used to have the equivalent voltage vectors, so it is possible to have an identical one on the ''abc'' board.

For the measurement of the reference currents, we shall proceed as follows: using theorem (5) and then (7), the reference speed shall give the reference torque expressed in function of the direct and transverse secondary stator current and the direct and transverse primary flux. This flux is also reflected in the function of the primary winding current. Based on this complex equation, the control method assumes that the direct current components are null and that only the transverse currents will be checked. It is, therefore, important to decouple the torque equation. As the function mode, using a four legs inverter is similar to two inverters are operated independently, the output power from the main inverter can be expressed in the equation (26). The maximum output power from this inverter is shown to be widely recognized by S_1.

$$\left(\frac{2}{3}S_1\right)^2 = \underbrace{\left[R_1 i_1^2 + \omega_{s,1} L_m i_1 i_2 \sin(\theta_{s,1} + \theta_{s,2})\right]^2}_{P_1} + \underbrace{\left[\omega_{s,1} L_1 i_1^2 + \omega_{s,1} L_m i_1, i_2 \cos(\theta_{s,1} + \theta_{s,2})\right]^2}_{Q_1} \tag{26}$$

Therefore, the cross-reference current of the main winding can be determined using equation (20). The final control scheme of this system will, therefore, be as set out in Figure (5). It is necessary to say that, in control, the scheme is based on equation (6) and not (7), the coupling effect does not occur, and each stator is regulated separately. The example is not used in an electric vehicle where, when the reference speed is set to 0; the engine must not be turned on. In this case, the computer will have a mechanical speed equal to $\omega_{s,1}$, which is usually an input equivalent of 50 Hz.

B. G2V RECHARGES SYSTEM: CONTROL SCHEME

As the vehicle will be charged from the grid, G2V, the full-bridge AC-DC bidirectional converter, serves as an active rectifier with sinusoidal current and unitary power factor during this operating period. The DC-DC converter is reversible and acts as a buck converter. To achieve the maximum amplitude of the individual current harmonics, defined by the IEC 61000-3-2 standard, it is necessary to synchronize the full-bridge AC-DC bidirectional converter controller with the fundamental voltage of the power grid. Therefore, the first algorithm that must be implemented by the digital controller is a single-phase Phase-locked Loop (PLL). This algorithm generates two sine-waves, 'α' and 'β', with a 90° change in unitary amplitude. When the PLL is synchronized with the power grid, the signal' α' corresponds to the fundamental voltage direct component of the power grid.

This signal is used as input to the digital control algorithms that followed[25]. The second control algorithm is

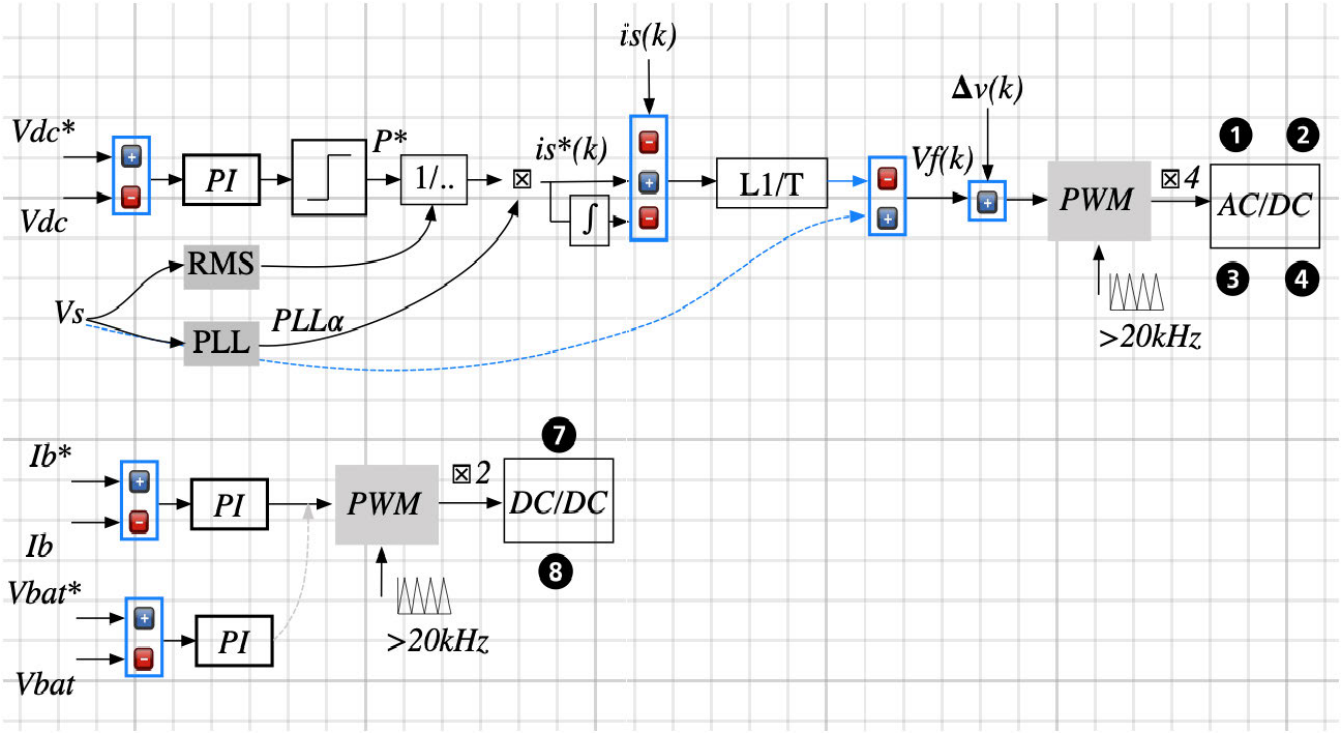

FIGURE 6. Control loop of the G2V recharge mode.

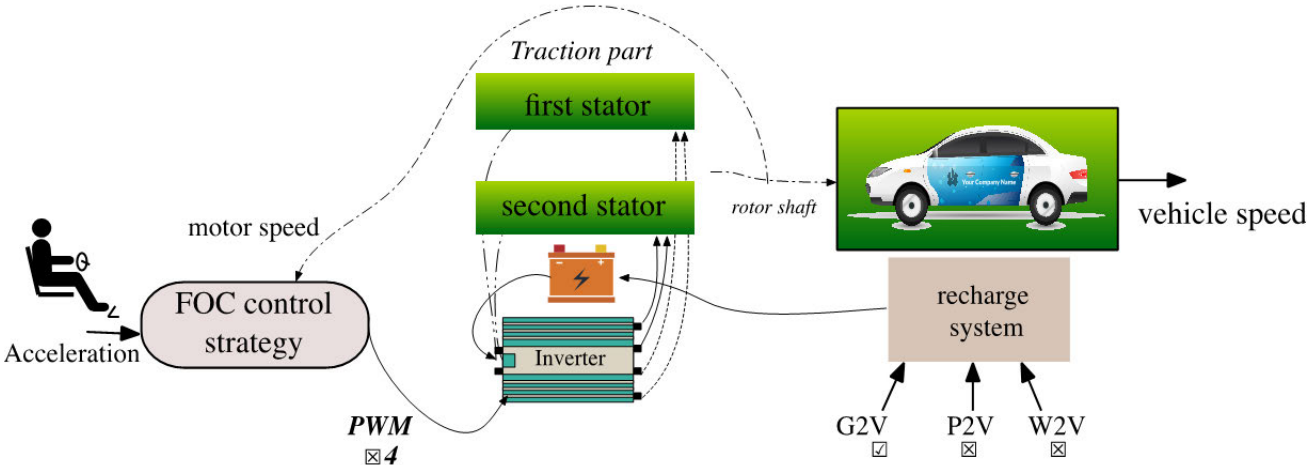

FIGURE 7. Blocks association for running EV simulations.

responsible for measuring the reference current for the bidirectional converter with full-bridge AC-DC. The amplitude of the reference current is determined by measuring the operating reference power by the power grid voltage, which is influenced by the' α' signal. The active reference power is obtained via a PI controller designed to keep the voltage of the DC link regulated. We note by $Vf(k)$ is the reference voltage, Vs (k) is the power grid voltage, is (k) is the full-bridge produced currents, the reference voltage calculated by the current control algorithm is applied to a unipolar sinusoidal Pulse Width Modulator (PWM). The control loop can be visualized in figure (6). In order to comply with the guidelines of the battery manufacturers, the reversible DC-DC converter is operated at both constant current and constant voltage levels, as shown in figure The relative current ($Ibat^*$) as compared to the actual current ($Ibat$) during the constant current level. The current error generated feeds the PI controller that changes the output duty cycle through a PWM modulator with a triangular carrier. When the maximum voltage value suggested by the battery manufacturer is reached, the control algorithm switches to a steady voltage point. A second PI controller is used at this stage to maintain a constant output

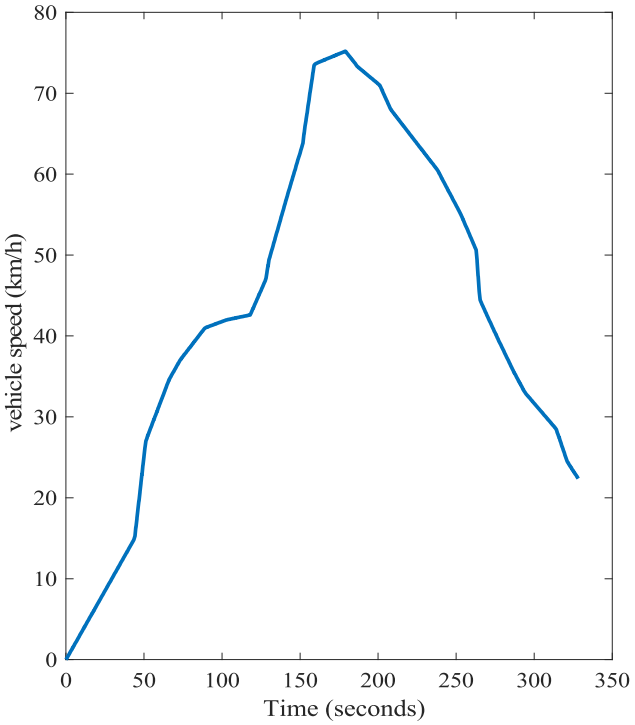

FIGURE 8. Vehicle speed according to the given acceleration form.

voltage (*Vbat*) of the reversible DC-DC converter according to the voltage reference (*Vbat**).

IV. CASE STUDY AND RESULTS IN DISCUSSION

All the mathematical models outlined in the preceding sections were implemented for all the blocks required. The global vehicle model was and is being developed in the MATLAB Simulink platform.

As shown in figure (7), the blocks are related. Also, the characteristics of the electric motor were fixed in order to drive a vehicle that has a weight equal to 700 kg and driven on a road that has a slop equal to 0%. A special acceleration form was given for driven the vehicle, as it is indicated in figure (9). In relation to the control organigram indicated in the figure (8), the control action will be applied to the traction system, precisely, on the electric motor, which has two separate stators. Before starting drawing the obtained results, we desire to expose the electrical specification of the used machine and the used battery. This is by showing they voltages, currants, and capacity, for the battery and the speed, torque, and voltage for the motor. Table (2), resumes the specifications of the engine, and specifically the parameters of the electric motor and battery pack. The condition of the road inside is also issued.

The simulation period of this test was applied in 300 seconds, devised into two parts. Firstly, an initial acceleration form was given in order to simulate a new drive cycle that can be found in the city. This drive cycle is characterized by different acceleration slopes for touching 70km/h as vehicle speed, split on 150 seconds. Then, a deceleration form was

TABLE 3. Electric vehicle specifications.

Double Stator Machine Parameters	Maximum Speed	5000 rpm
	Maximum Electric Power	30000 W
	Maximum Current	25/50 A
	Voltage	500 V
Battery Pack Characteristics	Voltage	220V
	The Initial State of Charge	67%
Vehicle and Road Specification	Vehicle Weight	700 kg
	Road Slope	0%
	Maximum Speed	80 km/h

given with various slopes, split on the rest of the simulation period. Figure (8), gives this reference form and shows the corresponding vehicle speed. It is important to indicate that the given acceleration form is the same as it is presented in the vehicle speed curve. The proportional factor between the two variable is 0,00438. A speed of 80 Km/h needs a 0,35% of acceleration ratio.

Depending on this acceleration criterion, the car speed must start from zero to 75 km / h in 180 seconds. This relation will, therefore, be used as the first input signal for the engine control unit, as shown in Figure (7). This feedback will be adjusted to the PWM reference signals for engine control by means of an analog four-leg inverter. The obtained engine speed will then be, as indicated in the figure (9). After feeding the two stators, this speed is reached by the required power. As shown in figure (9), when the engine speed reaches 2500 rpm, the second stator will be driven. A faster speed will be touched. The first stator to be fed was to help the vehicle achieve 42 km / h. Instead, when the speed of the car increases further, the second stator will be powered, and the engine will be able to touch higher speeds. It is likely, in reality, that the vehicle has higher speed than the average touched one since the usual speed of the electrical system is 5000 rpm.

We can also visualize this function mode in the stator current scheme. Fig (10) displays the two transverse currents in the two stator units. Initially, at the start mode, the first stator current touches 25 amperes, when the acceleration is maximum, then it stabilizes at 20 amperes when the second stator is started. The two stators are running ON, from 130 to 220 seconds. This will give more power for the vehicle, and this can also be visualized on the motor power scheme.

However, it is important to remember that the engine control loop does not include the optimum parameters of all the used controllers, and this can be demonstrated by the existing currents sharp pulse as the second stator begins. In fact, this effect must be avoided if the current sharp pulse across the nominal current value twice and for a long time. For this studied case, the current sharp pulse exists but not for a long time, so no risk exist and the system run perfectly. However,

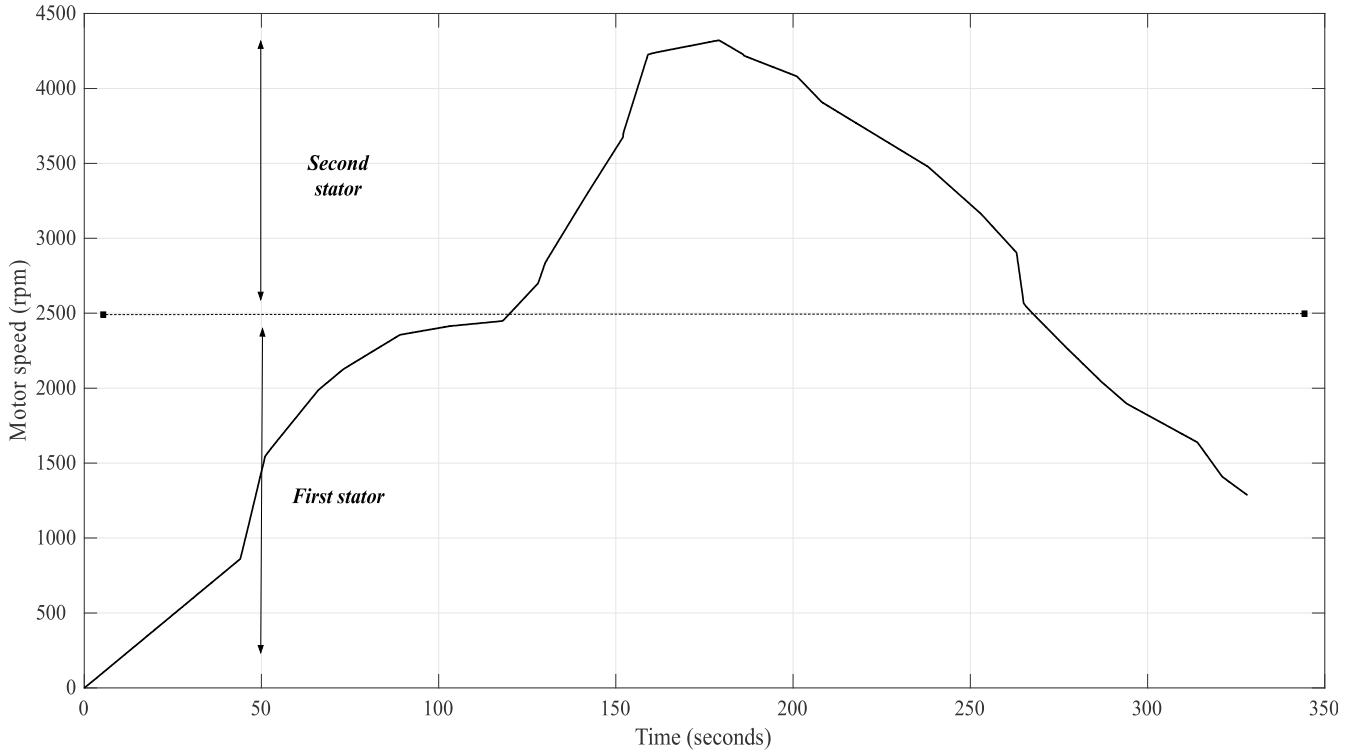

FIGURE 9. Electric motor speed.

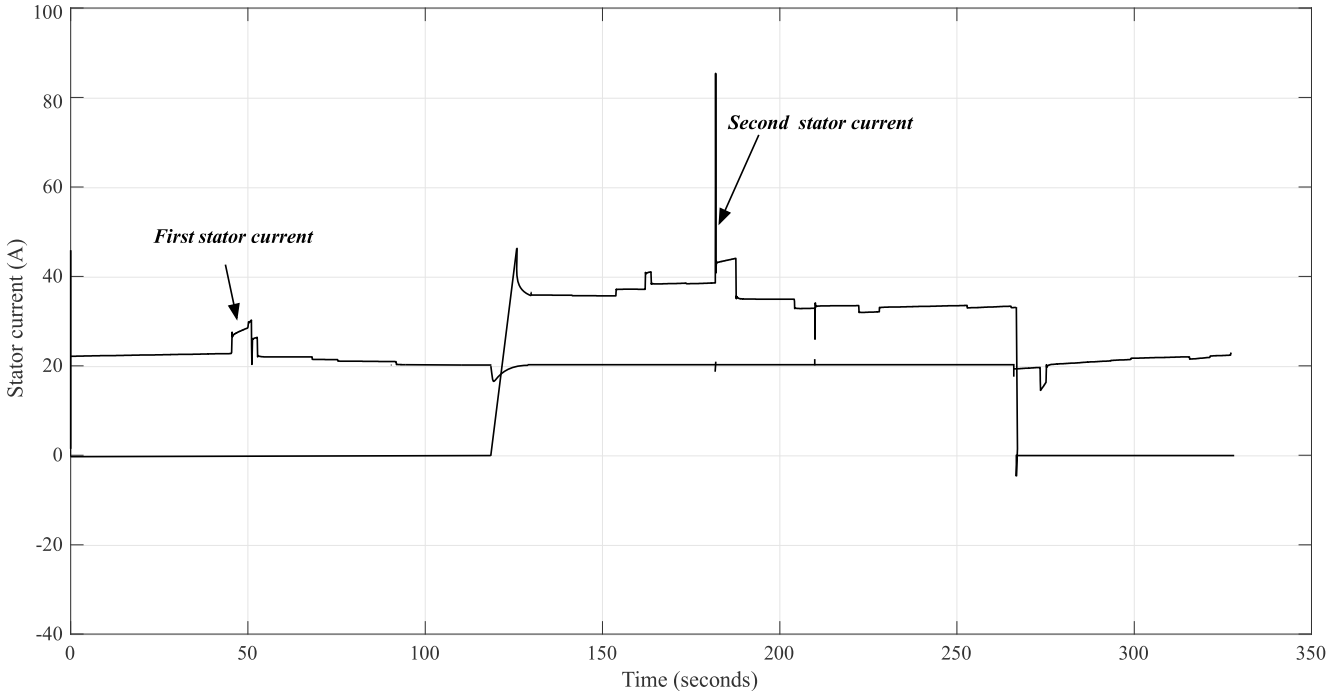

FIGURE 10. Stator currents.

using optimal current controls can increase the global engine efficiency, and these results can be improved by the PSO optimization toll.

The related engine power can also be visualized in Figure (11). This power reaches 15kW with the first stator and moves to 25kW after feeding the second stator.

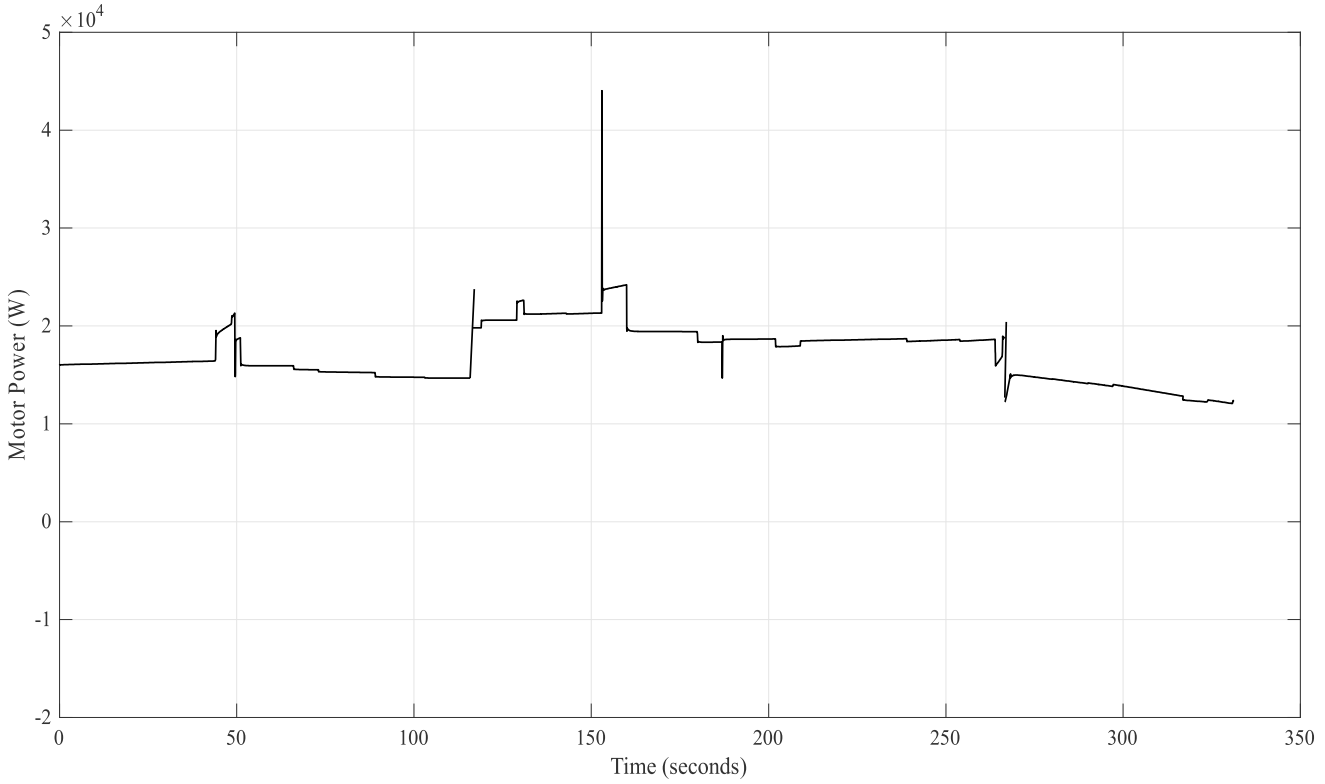

FIGURE 11. Motor power.

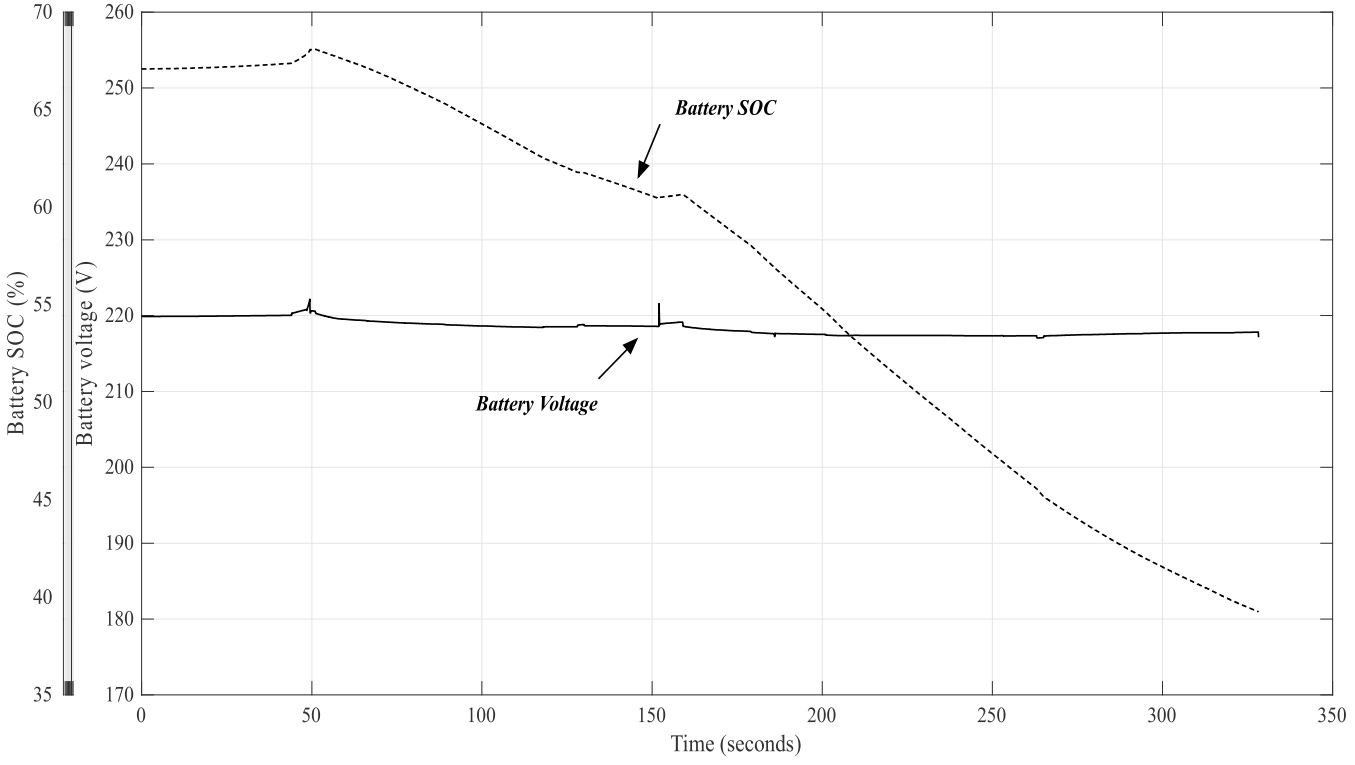

FIGURE 12. Battery voltage and battery SOC evolution.

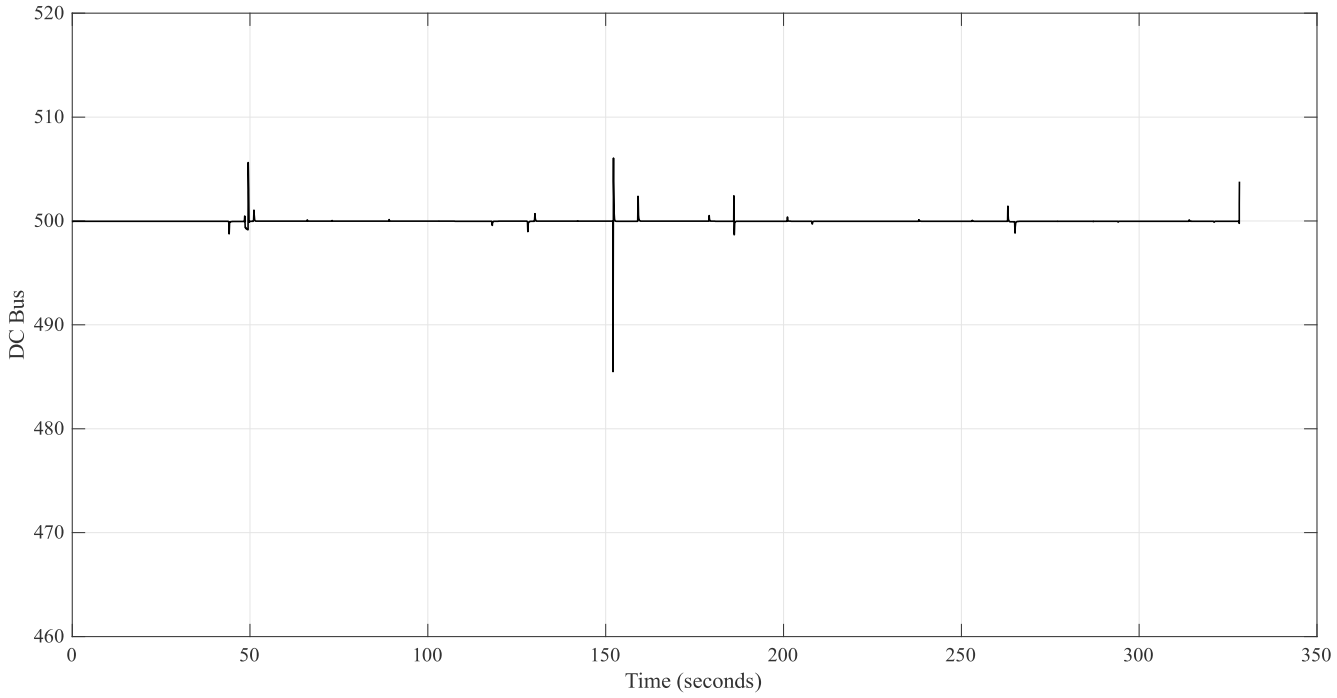

FIGURE 13. DC bus voltage from the inverter.

This amount of power is delivered from the battery pack. Figure (12) illustrates the battery statistics, as the battery voltage and the battery SOC. Actually, in this simulation, we have started with 67% as an initial battery SOC.

So, at the end of this simulation, the new SOC value is 38%. There is no recharging process in this running mode. Therefore, the SOC battery is still diminishing. Just a few positive picks occur in the transformation stages, which are confirmed by the momentum of the car when the maximum acceleration is modified to the lowest at an instant of 50 seconds and others.

We can also see that the battery voltage is still constant between 220 and 218 volts. This validates the reliability of the battery system configuration. But if the SOC battery drops more than the maximum value, the battery voltage would decrease further.

The adaptation between the battery voltage and the DC bus voltage on the inverter can also be visualized in figure (13). This one shows the stability of the DC voltage, which is fixed to 500 V.

V. CONCLUSION AND FUTURE ENDEAVORS

The work mentioned in this paper has been expanded to include mathematical analysis and has been translated into Simulink/MATLAB blocks. Other parameters, such as vehicle speed, motor speed, and others, were tracked and obtained after the overall system was run. Using the exposed control loops, we also implemented multiple PI controllers within the overall framework. In that related part, our remark about changing PI parameters was addressed. The PI parameters were modified by trial and error, and the results were satisfactory. Nonetheless, by presenting a list of guidelines in this section for the future use of methods and resources to boost the vehicle's overall performance, these results may be improved. These kinds of recommendations include a list of possible steps and questions to pursue in the future. The PSO programme and BFO system are referenced while using the optimization algorithm to adjust the PI parameters. [26], [27] include some helpful references. Also and after concentrating on another problem, researchers can work on other technics of motor control as this machine is not very knower, and its control methods are not all discovered. Maybe, having more precise mathematical models for the essential components inside the vehicle will help discovering the real power map inside the vehicle and can help next for managing the power inside and then can found other solutions for ameliorating vehicle autonomy.

As the presented analysis offers an education on the charging mechanism for an electric car, it is possible to extend the present work by including more possible solutions suited to the charging system. But, working on the control loop for assuring the overall recharge system stability can be a useful solution for the side of the vehicle and the side of the energy-exporting part as the grid section [28].

We will restart the exposed application in this section at the end of this segment so that the contribution can be explained as soon as possible. This paper also considers the analysis of the transportation system, with an emphasis on the pure electric car version. It defined and introduced the internal components. The mathematical models were also

developed and detailed in order to provide information about the inner parameters that operate the components as a whole. The battery pack was used because it is the system's main power source. Since this paper is about a particular electrical machine, a large portion of the study was devoted to describing the principles and requirements of electrical machines. The working mode of the corresponding mathematical model was given and defined in detail. The control actions and procedures used for efficient traction phases within a pure electric vehicle are also discussed in another section of this revision. A four-legged special inverter was used to create the control system. In addition, to operate a computer using field-oriented vector control, a special control system is designed and implemented. After obtaining all of the required components, a simulation process was started to test the control loop of this specific machine's reliability. A special drive loop was used in this simulation to achieve such high speeds and show the two stators' working modes. The currents of the stator, the voltage of the engine and the rpm were given and discussed for the presentation of the two phases of the power supply.

REFERENCES

[1] K. E. Brown and R. Dodder, "Energy and emissions implications of automated vehicles in the U.S. Energy system," *Transp. Res. D, Transp. Environ.*, vol. 77, pp. 132–147, Dec. 2019.

[2] A. M. Lulhe and T. N. Date, "A technology review paper for drives used in electrical vehicle (EV) & hybrid electrical vehicles (HEV)," in *Proc. Int. Conf. Control, Instrum., Commun. Comput. Technol. (ICCICCT)*, Dec. 2015, pp. 632–636.

[3] N. Patin, "2-DC/AC converters," in *Power Electronics Applied to Industrial Systems and Transports*, vol. 2, T. Patin, Ed. Amsterdam, The Netherlands: Elsevier, 2015, pp. 35–100.

[4] Y. Luo, C. Liu, F. Yu, and C. H. T. Lee, "Design and evaluation of an efficient three-phase four-leg voltage source inverter with reduced IGBTs," *Energies*, vol. 10, no. 4, p. 530, Apr. 2017.

[5] M. Shahbazi, M. R. Zolghadri, P. Poure, and S. Saadate, "Wind energy conversion system based on DFIG with open switch fault tolerant six-legs AC-DC-AC converter," in *Proc. IEEE Int. Conf. Ind. Technol. (ICIT)*, Feb. 2013, pp. 1656–1661.

[6] D. Rezzak and N. Boudjerda, "Management and control strategy of a hybrid energy source fuel cell/supercapacitor in electric vehicles," *Int. Trans. Electr. Energy Syst.*, vol. 27, no. 6, p. e2308, Jun. 2017.

[7] N. Mohamed, F. Aymen, M. Ben Hamed, and S. Lassaad, "Analysis of battery-EV state of charge for a dynamic wireless charging system," *Energy Storage*, vol. 2, no. 2, pp. 1–10, Apr. 2020.

[8] A. Flah and C. Mahmoudi, "Design and analysis of a novel power management approach, applied on a connected vehicle as V2 V, V2B/I, and V2N," *Int. J. Energy Res.*, vol. 43, no. 8, pp. 1–21, 2019.

[9] K. A. Chinmaya and G. K. Singh, "Experimental analysis of various space vector pulse width modulation (SVPWM) techniques for dual three-phase induction motor drive," *Int. Trans. Electr. Energy Syst.*, vol. 29, no. 1, Jan. 2019, Art. no. e2678.

[10] A. Flah, A. K. Irfan, A. Agarwal, L. Sbita, and G. S. Marcelo, "Field-oriented control strategy for double-stator single-rotor and double-rotor single-stator permanent magnet machine: Design and operation," *Comput. Electr. Eng.*, vol. 90, pp. 1–15, Mar. 2021.

[11] Y. Wang, Y. Sun, Y. Wang, and X. Zhang, "Simulation of dual-stator permanent magnet synchronous motor for electric vehicle," in *Proc. IEEE Adv. Inf. Manage., Communicates, Electron. Autom. Control Conf. (IMCEC)*, Oct. 2016, pp. 1430–1433.

[12] R. E. Betz and M. G. Jovanović, "Introduction to the space vector modeling of the brushless doubly fed reluctance machine," *Electr. Power Compon. Syst.*, vol. 31, no. 8, pp. 729–755, Aug. 2003.

[13] X. Guo, S. Wu, W. Fu, Y. Liu, Y. Wang, and P. Zeng, "Control of a dual-stator flux-modulated motor for electric vehicles," *Energies*, vol. 9, no. 7, p. 517, Jul. 2016.

[14] X. Wei, M. Cheng, W. Wang, P. Han, and R. Luo, "Direct voltage control of dual-stator brushless doubly fed induction generator for stand-alone wind energy conversion systems," *IEEE Trans. Magn.*, vol. 52, no. 7, pp. 1–4, Jul. 2016.

[15] K. Matsuse, N. Kezuka, and K. Oka, "Characteristics of independent two induction motor drives fed by a four-leg inverter," *IEEE Trans. Ind. Appl.*, vol. 47, no. 5, pp. 2125–2134, Sep. 2011.

[16] S. Lee, J. Cherry, M. Safoutin, J. McDonald, and M. Olechiw, "Modeling and Validation of 48V Mild Hybrid Lithium-Ion Battery Pack," *SAE Int. J. Altern. Powertrains*, vol. 7, no. 3, pp. 1–11, 2018.

[17] D. Zhou, F. Gao, A. Ravey, A. Al-Durra, and M. G. Simoes, "Online energy management strategy of fuel cell hybrid electric vehicles based on time series prediction," in *Proc. IEEE Transp. Electrific. Conf. Expo (ITEC)*, Jun. 2017, pp. 113–118.

[18] R. Zhang, J. Tao, and H. Zhou, "Fuzzy optimal energy management for fuel cell and supercapacitor systems using neural network based driving pattern recognition," *IEEE Trans. Fuzzy Syst.*, vol. 27, no. 1, pp. 45–57, Jan. 2019.

[19] A. Ul-Haq, C. Cecati, and E. A. Al-Ammar, "Modeling of a photovoltaic-powered electric vehicle charging station with vehicle-to-grid implementation," *Energies*, vol. 10, no. 1, pp. 1–20, 2017.

[20] Y. J. Jang, Y. D. Ko, and S. Jeong, "Optimal design of the wireless charging electric vehicle," in *Proc. IEEE Int. Electr. Vehicle Conf.*, Mar. 2012, pp. 1–5.

[21] M. Naoui, A. Flah, and M. Ben hamed, "Inductive charger efficiency under internal and external parameters variation for an electric vehicle in motion," *Int. J. Powertrains*, vol. 8, no. 4, pp. 343–358, 2019.

[22] P. Gao, Y. Gu, and X. Wang, "The design of a permanent magnet in-wheel motor with dual-stator and dual-field-excitation used in electric vehicles," *Energies*, vol. 11, no. 2, p. 424, Feb. 2018.

[23] M. Hasoun, A. El Afia, and M. Khafallah, "Field oriented control of dual three-phase PMSM based vector space decomposition for electric ship propulsion," in *Proc. Int. Conf. Comput. Sci. Renew. Energies (ICCSRE)*, Jul. 2019, pp. 1–6.

[24] G. A. Parameswari and H. H. Sait, "A comprehensive review of fault ride-through capability of wind turbines with grid-connected doubly fed induction generator," *Int. Trans. Electr. Energy Syst.*, vol. 30, no. 8, Apr. 2020, Art. no. e12395.

[25] J. G. Pinto, V. Monteiro, H. Goncalves, B. Exposto, D. Pedrosa, C. Couto, and J. L. Afonso, "Bidirectional battery charger with grid-to-vehicle, vehicle-to-grid and vehicle-to-home technologies," in *Proc. IECON 39th Annu. Conf. IEEE Ind. Electron. Soc.*, Nov. 2013, pp. 5934–5939.

[26] F. Aymen and S. Lassaad, "BFO control tuning of a PMSM high speed drive," in *Proc. 16th IEEE Medit. Electrotech. Conf.*, Mar. 2012, pp. 273–276.

[27] F. Aymen, M. Novak, and S. Lassaad, "An improved reactive power MRAS speed estimator with optimization for a hybrid electric vehicles application," *J. Dyn. Syst., Meas., Control*, vol. 140, no. 6, Jun. 2018, Art. no. 061016.

[28] S. Ou, Z. Lin, X. He, S. Przesmitzki, and J. Bouchard, "Modeling charging infrastructure impact on the electric vehicle market in China," *Transp. Res. D, Transp. Environ.*, vol. 81, Apr. 2020, Art. no. 102248.

FLAH AYMEN was born in Gabès, Tunisia, in 1983. He received the bachelor's and the M.Tech. degrees in electrical engineering from the National School of Engineers of Gabès (ENIG), Tunisia, in 2007 and 2009, respectively, and the Ph.D. degree from the Department of Electrical Engineering, in 2012. He has academic experience of 11 years. He has published over 40 research papers in reputed journals, international conferences, and book chapters. His research interests include electric vehicle, power systems, and renewable energy.

MAJED ALOWAIDI (Member, IEEE) received the B.Eng. (Hons.) degree from the Riyadh College of Technology, in 2006, and the M.A.S. and Ph.D. degrees in computer engineering from the University of Ottawa, Canada, in 2012 and 2018, respectively. He is currently working as an Assistant Professor and the Head of the IT Department, College of Computer and Information Science, Majmaah University, Majmaah, Saudi Arabia. He has been a member of MCRLAB, University of Ottawa, since 2012. His research interests include cybersecurity, the IoT, semantic web, cloud and edge computing, and smart city.

MOHIT BAJAJ (Member, IEEE) was born in Roorkee, India, in 1988. He received the bachelor's degree in electrical engineering from the FET, Gurukula Kangri Vishwavidhyalya, Haridwar, India, in 2010, and the M.Tech. degree in power electronics and ASIC design from NIT Allahabad, Uttar Pradesh, India, in 2013. He is currently pursuing the Ph.D. degree with the Department of Electrical and Electronics Engineering, NIT Delhi, India. He has academic experience of five years. He has published over 30 research articles in reputed journals, over 30 research papers in international conferences, and book chapters. His research interests include power quality improvement in renewable DG systems, distributed generations planning, application of multi-criteria decision making in power systems, custom power devices, the IoT, and smart grids.

NAVEEN KUMAR SHARMA (Senior Member, IEEE) received the B.Tech. degree in electrical and electronics engineering from Uttar Pradesh Technical University, Lucknow, Uttar Pradesh, in 2008, the M.Tech. and Ph.D. degrees in power system from National Institute of Technology, Hamirpur, India, in 2010 and 2014, respectively. He worked as a Lecturer with the Department of Electrical Engineering, National Institute of Technology, Hamirpur, Himachal Pradesh, from March 2014 to May 2017. He is currently an Assistant Professor with the Department of Electrical Engineering, I. K. G. Punjab Technical University, Kapurthala, Punjab. He has published several research papers in leading international journals and conference proceedings, and presented papers at several prestigious academic conferences, such as IEEE and Springer. His research interests include power market, renewable energy sources, power system optimization, and condition monitoring of transformers.

SHAILENDRA MISHRA (Senior Member, IEEE) received the Master of Engineering (M.E.) and Ph.D. degrees in computer science and engineering from the MotiLal Nehru National Institute of Technology (MNNIT), India, in 2000 and 2007, respectively. He is currently working as an Associate Professor with the Department of Computer Engineering, College of Computer and Information Science, Majmaah University, Majmaah, Saudi Arabia. He published and presented more than 90 research papers in international journals and international conferences. His recent research interests include cloud and cyber security, SDN, and the IoT Security also conducting research on communication system and computer networks with performance evaluation and design of multiple access protocol for mobile communication networks. He is also a Senior Member of ACM, a Life Member of the Institution of Engineers India (IEI), the Indian Society of Technical Education (ISTE), and ACEEE.

SUNIL KUMAR SHARMA received the Ph.D. degree in mathematics from Gautam Buddh Technical University, Lucknow, India. He is currently an Associate Professor of mathematics with the College of Computer and Information Sciences. Majmaah University, Saudi Arabia. His research interests include deal with the cloud security, mathematical modelling, numerical computation of biomechanics of diarthrodial joints, multicriteria decision model for production systems, robot in the field of education, and cloud security. His current research interest includes mathematical modelling of physical and biological problems in general and mathematical analysis. He is also a member of AMC.